ELSEVIER

International Journal of Heat and Fluid Flow 20 (1999) 486–491

International Journal of HEAT AND FLUID FLOW

www.elsevier.com/locate/ijhff

Experimental investigation of dynamic binary collision of ethanol droplets – a model for droplet coalescence and bouncing

J.-P. Estrade *, Hervé Carentz, G. Lavergne, Y. Biscos

ONERA-CERT, 2 Avenue Edouard Belin, 31055 Toulouse Cedex 04, France

Abstract

Binary droplet collisions are studied by means of an experimental set-up, which permits one to obtain accurate measurements (within 10% error) of droplet number, sizes and velocities. Ethyl alcohol droplet collisions have been investigated for distinct diameter ratios $\Delta = 1$ and $\Delta = 0.5$. Different domains of collision outcome are brought out. Transition curves in the literature are compared to the present experimental data. A new theoretical prediction of bouncing is proposed and compared with experimental values. Quantitative measurements of droplet velocities after impact are also obtained. A model to predict droplet velocities for coalescence and bouncing is presented. Droplet sizes and velocities when separation occurs are also given and discussed.

Notation

d_l	initial droplet large diameter
d_s	initial droplet small diameter
Ec_d	kinetic energy of deformation
Ec_e	stretching kinetic energy
E_{rot}	rotational energy
Es_f	surface tension energy of deformed drops
Es_i	surface tension energy of the initial two drops
h_l	deformed large droplet height
h_s	deformed small droplet height
I	non-dimensional impact parameter
Oh	Ohnesorge number
Re	Reynolds number
r_l	large deformed droplet radius
V_{Li}	large drop interaction region volume
r_s	small deformed droplet radius
V_r	droplet relative velocity
We	Weber number
Greek	
δ	dimensional impact parameter
μ	droplet viscosity
ϕ	shape parameters
ω	interaction region width
ρ	droplet density
σ	surface tension coefficient
τ	defined as $(1 - I)(1 + \Delta)$
Δ	diameter ratio

1. Introduction

Spray structure is greatly affected by drop collisions. Due to very complex physical phenomena involved in the process, research has been mainly directed at qualitative experiments. The purpose of the present experimental study is to obtain a model for droplet collision. To reach this point, two main problems need to be solved. The first consists of determining accurate transition curves between all binary collision outcomes; the second is to develop a new model, based on experimental data, to predict droplet velocities and sizes after impact for each outcome.

The literature is quite rich in papers on qualitative aspects of collision. According to most studies, binary droplet collisions exhibit five distinct collision regimes named coalescence with minor deformation (I), bouncing (II), coalescence with major deformation (III), reflexive deformation (IV), and rotational or stretching separation (V).

To characterise the collision process, many authors use the Weber number We, and the impact parameter I respectively, defined by

$$\mathrm{We} = \frac{\rho d_s V_r^2}{\sigma}, \tag{1}$$

$$I = \frac{2\delta}{d_l + d_s} \tag{2}$$

with δ described in Fig. 1.

Brazier-Smith et al. (1972) as well as Poo (1990) introduces also the diameter ratio Δ defined as the ratio d_s to d_l. Almost the whole work on drop collision has consisted of determining transition curves between these distinct regimes. Brazier-Smith proposed in 1968, a theoretical boundary curve between regimes (III) and (V) taking into account Δ, I and We. He also puts forward a boundary curve between regimes (II) and (III) but this has never been compared to experimental data.

* Corresponding author. E-mail: jean-philippe.estrade@onecert.fr

0142-727X/99/$ – see front matter
PII: S0142-727X(99)00036-3

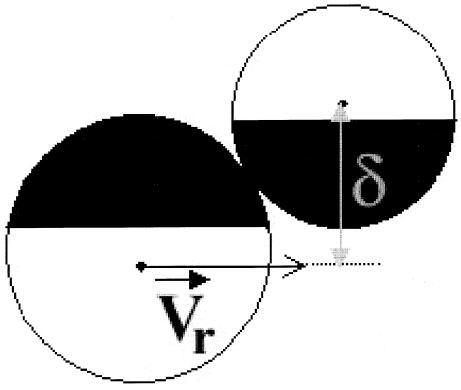

Fig. 1. Definition of dimensional impact parameter δ and interaction volumes.

More recently, Poo has obtained a transition curve between regimes (III) and (V). He has proposed the only existing transition curve to distinguish coalescence (III) from separation at low impact parameter (IV).

Another parameter affects the droplet collision process, the liquid viscosity μ. In the past, many authors have noted the influence of μ but Qian and Law (1994) alone give experimental results of the influence of μ which can be taken into consideration in terms of the Ohnesorge number Oh defined by Eq. (3).

$$\mathrm{Oh} = \frac{\mu}{\sqrt{\sigma \rho d_s}}. \tag{3}$$

Qian et al. demonstrate the linear evolution of the boundary curve between (III) and (IV) as a function of Oh. Their correlation permits the connection with the transition Weber number We_2 between regimes (III) and (IV) with Oh. We_2 is defined as the transitional Weber number between regimes (III) and (IV) when $I=0$, like We_1 represents the critical Weber number between regimes (II) and (III) and We_0 between regimes (I) and (II). Jiang et al. (1991) has also shown that critical Weber numbers We_0, We_1 and We_2 vary linearly with μ/σ ratio. Jiang's linear correlation possesses the drawback of not taking into account any diameter scale but, on the other hand, it describes the evolution of all the critical Weber numbers We_0, We_1 and We_2.

In the present paper, a synthesis of the works done by Qian, Poo, Brazier-Smith et al. and Jiang is presented with the present boundary curve to predict bouncing are compared to experimental measurements.

Menchaca-Rocha et al. (1994) were the first to report a quantitative study of droplet collision. He gives the number and sizes distribution of drops produced by regime (V) when $\Delta = 1$. Besides, in a recent paper, Brenn et al. (1998) presented many results on the production of satellite droplets when stretching separation occurs. These interesting results are compared and discussed together with our own.

2. Experimental set-up

The whole experimental set up is described in Fig. 2. Periodical break-up of two liquid jets, which converge in the same vertical plane, produces streams of equally spaced and uniformly sized drops that collide in a repeat fashion. This device consists of a capillary tube, a piezoelectric ceramic and an exit orifice. The ethanol reservoir, which is pressurised by a 100-liter air-tank, supplies the injector by forcing the liquid through the capillary tube. The piezoelectric ceramic vibrates while excited by a function generator. The mechanically induced vibration causes the disintegration of the liquid jet due to Rayleigh instability. Each injector is fitted to a mechanical support system. This support is connected to a micro-metric plate allowing it to be moved up and down. Thus, one can modify the droplet stream offset. Additionally, micro-metric plates are positioned on two distinct mechanical arms which possess the same rotation axis. So, one can adjust the angle between the two jets. Finally, one of the injectors is also equipped with another rotation micro-metric displacement system to adjust the two stream positions in the same plane, which we term the collision plane.

The orifice diameter, the air-tank pressure, the generator frequency, the two-jet angle and finally the relative vertical injector position define droplet sizes, velocities and impact parameter.

By adjusting both the air-tank pressure and the generator frequency, a uniform stream of droplets can be produced. The observation technique is shadowgraphy. A permanent light source is used. To get a still image by means of an intensified video camera associated with a zoom system, the use of a shutter driven by a shutting generator synchronised with the frequency generator is required. To obtain a high-resolution quality, the collision phenomenon is decomposed into several images. The whole phenomenon is then reconstructed (Fig. 3) through a specific software developed with visual C++ 4 language.

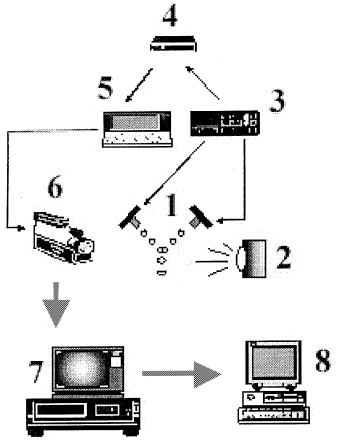

1. Specific injectors.
2. Continuous light source (ORIEL lamp).
3. Function generator.
4. Electronics system for synchronisation.
5. Shutting generator.
6. Intensified video camera.
7. Monitor and video recorder.
8. Computer.

Fig. 2. Schematic description of the experimental set-up.

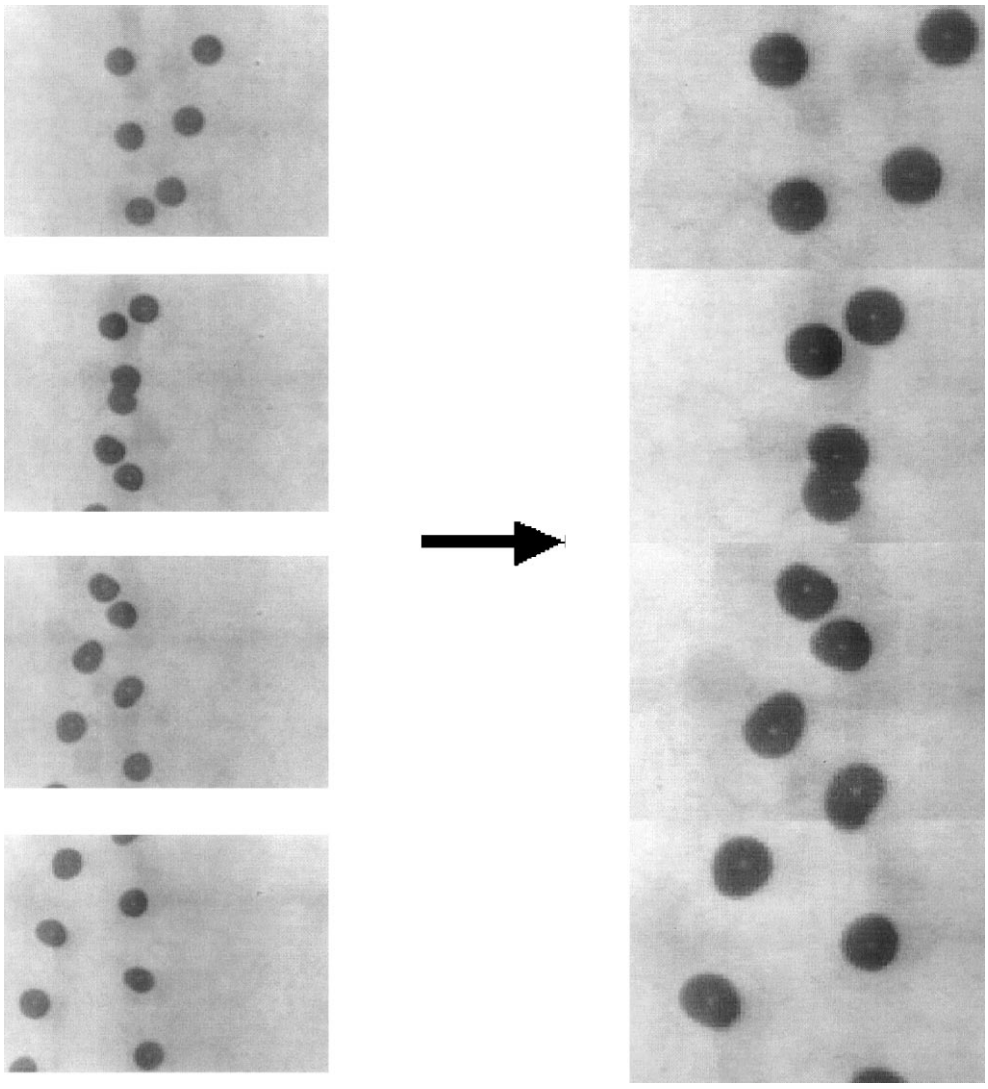

Fig. 3. Reconstruction of the integral collision process from several recorded images.

The vertical position of the camera must be set in order to obtain an image of the two droplet streams just before impact. It allows initial conditions of impact (We, I, Δ) measurements. Such information is given by the specific software. Then, the following images, obtained by moving down the camera, are recorded on a video recorder for post-experiment image treatment. Thanks to the vertical displacement camera system, looking down along the converging stream means going downward in the collision process. Due to low fluctuations of the initial conditions, the time-base image treatment is entirely feasible but can be extremely time consuming.

The measurement technique described here provides impact initial conditions (diameters, velocities) likewise the resulting droplet number, velocities and diameters within 10% error.

The results presented in this paper have been obtained by conducting experiments on ethanol droplets colliding at atmospheric pressure. Their diameters range from 80 to 300 μm and their velocities vary from 3 to 12 m/s. Considering ethyl alcohol properties and the impact initial conditions explored, the Reynolds number ranges from 132 to 791. It does not appear to exert a real influence on the investigated results of collision. Due to experimental constraints, low Weber numbers could not be explored. In fact, for relatively low velocity injection, a stable break-up of the liquid jet is impossible to generate.

3. Results

Qualitative results in terms of collision regime are shown in Figs. 4 and 5 for ethyl alcohol.

Experimental data presented permit the different collision outcomes to be brought out. Regime (V) shows a wide range of satellite drops produced by rupture. It is really a very unstable phenomenon. A small perturbation of initial conditions results in a very different number of satellites. However, a domain corresponding to separation with production of one satellite appears in Fig. 4. No attempt to characterise the boundaries has been made. One can note that separation with production of one satellite is the major event for $\Delta = 1$ whereas it is less uncommon for $\Delta = 0.5$. In this case, separation without satellite appears to be very frequent (Fig. 5).

A new theoretical curve (C_1), whose equation is presented in the next section, is used to predict bouncing. It fits very well with experimental data for $\Delta = 1$ as well as $\Delta = 0.5$. Curve (C_1) intercepts the axis for $We = We_1$ (Figs. 4 and 5). This value has

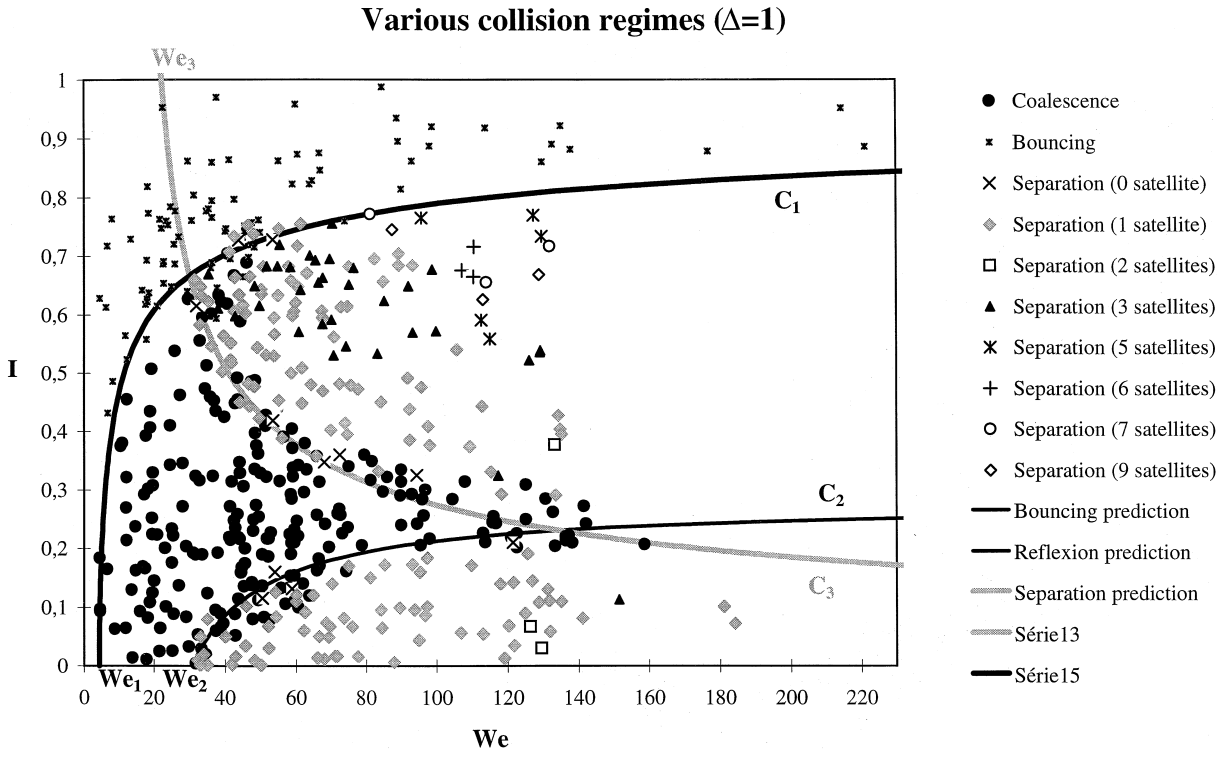

Fig. 4. Analytically obtained regions of different collision outcomes for drop size ratio $\Delta = 1$, together with experimental data.

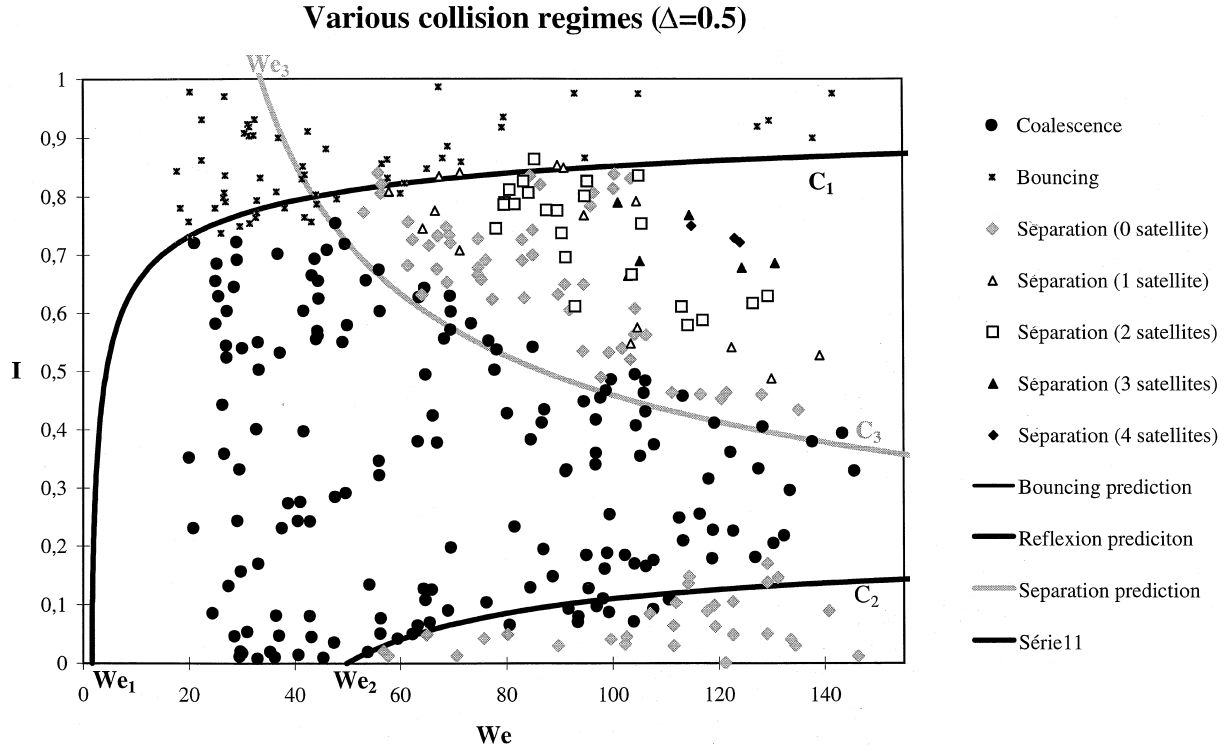

Fig. 5. Analytically obtained regions of different collision outcomes for drop size ratio $\Delta = 0.5$, together with experimental data.

been chosen according to experimental results but is in quite good agreement with Jiang's correlation. This predicts for ethyl alcohol ($\mu/\sigma = 0.053$), $We_1 = 2.8$ whereas measurements give $We_1 = 4.57$ for $\Delta = 1$. The Brazier-Smith (Brazier-Smith et al., 1972) correlation for predicting bouncing is in complete disagreement with our experimental data.

Poo's curve (C_2) also agrees relatively well with experiments when corrected according to Qian's law. This later permits the

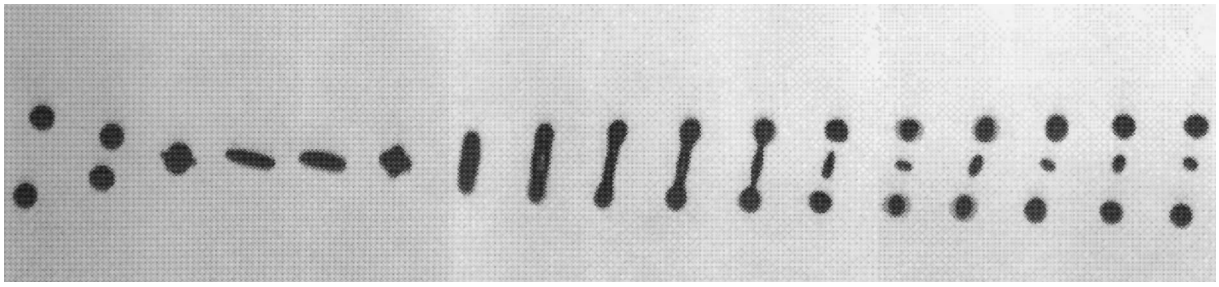

Fig. 6. Example of reflexive separation.

calculation of We_2 thanks to the simple knowledge of the Ohnesorge number. The simultaneous use of Poo's curve (C_2) and Qian's predicts respectively, for $\Delta = 1$ and $\Delta = 0.5$, $We_2 = 28.4$ and $We_2 = 46.7$ when our measurements give $We_2 = 30.6$ and $We_2 = 49.7$ for the same cases.

The prediction of separation at high impact parameter is best obtained with the Brazier-Smith (Brazier-Smith et al., 1972) boundary curve when modified as follows. The Brazier-Smith equation is determined while assuming that break-up occurs when rotational energy of the temporary coalesced drop exceeds the surface energy required to maintain the droplet in its single state. Brazier-Smith et al. calculated the moment of inertia of the unified droplet just after impact assuming a spherical shape while phenomenological observation shows a disk with rounded ends. By correcting the moment of inertia taking into account our experimental data, curve (C_3) agrees quite well with the boundary curve between (III) and (IV). However, one can note a relatively high discrepancy for smaller values of the impact parameter. Indeed, Brazier-Smith et al. only take into account the rotational energy of the temporally coalesced drop to explain separation. This rotational energy should not be so essential when I is low.

On the other hand, video observation tends to agree with Poo's analysis of separation for high I. According to him break-up occurs due to stretching of the unified initial droplets. The white portion of drops (Fig. 1) induces stretching and promotes separation. Nevertheless, the boundary curve proposed by Poo is in less agreement even for low impact parameters.

Quantitative results in terms of droplet velocities and sizes for coalescence and bouncing are compared to very simple models. For coalescence, the measured droplet velocity is compared to the calculated velocity evaluated while assuming momentum conservation. For bouncing, it is compared to droplet velocities as if there is no modification caused by interaction. The model for coalescence agrees with our experimental data. Comparison of the calculated and measured droplet velocities give a small gap (less than 10%). This tends to increase when We becomes greater but values remain low. Indeed, greater Weber number causes more momentum transferred to the gas principally because of the bigger deformation just after impact.

The bouncing investigation proves that droplets are little affected. A comparison of measured and calculated velocities shows very small differences (less than 10%). The smaller I, the greater this discrepancy. Indeed, as the impact parameter decreases, droplets are more influenced by bouncing as they undergo greater deformation while colliding. However, the gap remains relatively small. The experimental set-up only permits bouncing to be exhibited for quite large impact parameters larger than 0.3.

One can note that Fig. 4 is quite similar to the results obtained by Brenn et al. For separation, sufficient quantitative measurements have been obtained of both velocities and sizes for separation with formation of one or no satellite. These are now discussed. Break-up without the formation of satellites generates the primary two drops for both reflexive separation (IV) and regime (V). Menchaca-Rocha et al. noticed the same phenomenon. For $\Delta = 0.5$, the two drops produced by collision possess the same diameter ratio. Post-collision droplet velocity moduli are identical. Separation with formation of one satellite generates different droplet sizes when regime (IV) or (V) occurs. For regime (IV) break-up produces two twin-drops located on both sides of the smaller satellite whose diameter represents 26% of the total mean diameter of the two initial droplets. In contrast, regime (V) produces a satellite drop whose diameter is only 17%. Experiments have also revealed that the twin-droplet velocity for regime (V) corresponds to the initial droplet velocities. They conserve their direction whereas the satellite droplet velocities direction is different and approximately equivalent to the bisecting line of the twin-drop trajectories. However, for regime (IV) the velocities of the three drops are identical to the initial mean velocity. Reflexive separation leads to the production of three droplets whose directions are parallel. The satellite is located between the twin-drops and the distance between them corresponds to the maximum length of the stretched filament just before break-up (Fig. 6). Other quantitative results on separation are still insufficiently numerous to be discussed. Finally, no model for separation is yet proposed.

4. Theoretical prediction of bouncing

We have performed an energy balance to get a new boundary curve to predict bouncing. Experimental observation shows that when bouncing apart, spherical droplets roughly transform into a portion of a sphere. The criterion for bouncing is that the droplet initial kinetic energy of deformation as defined by Eq. (4), does not exceed the energy required to produce a limit deformation (Fig. 7). The droplet binary collision is written in terms of the mass centre coordinates of the smaller droplet. Taking into account the short delay time needed to produce the deformation observed when

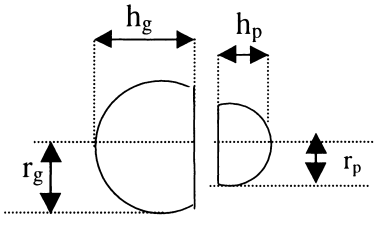

Fig. 7. Model of droplet deformation when bouncing according to experimental observations.

rebound occurs, it is reasonable to assume that no energy exchange exists between gas and droplets and that there is no viscous dissipation. The energy balance is defined by the following equation,

$$\mathrm{Ec_e} + \mathrm{Ec_d} + \mathrm{Es_i} = \mathrm{Es_f} + E_{\mathrm{rot}}. \tag{4}$$

The initial kinetic energy of the interaction region (black portion of Fig. 1) which contributes to the deformation is given by

$$\mathrm{Ec_d} = \frac{1}{2}\rho\left(V_{\mathrm{Li}}(U_s\cos\theta)^2\right) \tag{5}$$

with $\sin\theta = I$, where θ is the angle between the centre-to-centre line and the relative velocity vector $\vec{U}$ in R coordinates system.

$$V_{\mathrm{Li}} = \chi_1\frac{\pi d_l^3}{6}$$

is defined by the following equations,

$$\chi_1 = \begin{cases} \left(1 - \frac{1}{4}(2-\tau)^2(1+\tau)\right) & \text{for } \omega > \frac{d_l}{2}, \\ \frac{1}{4}\tau^2(3-\tau) & \text{for } \omega \leqslant \frac{d_l}{2} \end{cases}$$

with $\tau = (1-I)(1+\Delta)$. ω is the width of the overlapping interaction region (Fig. 1)

$$\omega = \left(\frac{d_s + d_l}{2}\right)(1-I).$$

The initial surface tension energy is equal to $\mathrm{Es_i} = \sigma\pi\left(d_s^2 + d_l^2\right)$.

The final surface tension energy can be written as

$$\mathrm{Es_f} = \sigma\pi\left(\frac{2h^2}{3} + \frac{1}{3}\frac{d_l^3}{h}\right) + \sigma\pi\left(\frac{2h'^2}{3} + \frac{1}{3}\frac{d_l^3}{h'}\right).$$

Bouncing occurs when $h_s \leqslant \phi r_s$ and $h_l \leqslant \phi r_l$ where ϕ is defined as the ratio h_s/r_s or h_l/r_l beyond which coalescence or separation occurs.

These conditions and the mass conservation of the two droplets permit the following relations to be written

$$h_l \leqslant d_l\left(\sqrt[3]{3/\phi^2 + 1}\right), \quad h_s \leqslant d_s\left(\sqrt[3]{3/\phi^2 + 1}\right).$$

$\mathrm{Es_f}(h_s, h_l)$ is an monotonically increasing function as experimental observations bring out that h_s/r_s and h_p/r_p together are greater than 1. So $h_s \leqslant \phi r_s$ and $h_l \leqslant \phi r_l$ give the following equation,

$$\mathrm{Es_f} \geqslant (1/3)\sigma\pi d_g^2(1+\Delta^2)\left(2\left(3/\phi^2+1\right)^{-2/3} + \left(3/\phi^2+1\right)^{1/3}\right).$$

Assuming $E_e = E_{\mathrm{rot}}$, the energy balance (4) gives

$$\mathrm{Ec_d} \geqslant \sigma\pi d_l^2/3(1+\Delta^2)\left(2\left(3/\phi^2+1\right)^{-2/3} + \left(3/\phi^2+1\right)^{1/3}\right) - \sigma\pi d_l^2(1+\Delta^2).$$

using Eq. (5), we obtain

$$\mathrm{We} \geqslant \frac{\Delta\left(1+\Delta^2\right)(4\phi' - 12)}{(\chi_1)(\cos\ (\arcsin I))^2} \tag{6}$$

with $\phi' = 2\left(3/\phi^2+1\right)^{-2/3} + \left(3/\phi^2+1\right)^{1/3}$. Eq. (6) represents the equation of the curve (C_1).

5. Conclusion

We have performed an experiment useful for the study of binary droplet collision. A new theoretical boundary curve to predict bouncing is also proposed and appears to fit very well with our experimental data. The synthesis of the literature works together with our results permit each collision regime to be predicted, according to liquid properties. Further experiments with various liquids will be undertaken to definitively validate the model. A new model to calculate droplet velocities when bouncing or coalescing has been tested and adopted. More experimental data are necessary to determine velocities and sizes of droplets for regimes (IV) and (V) while considering initial conditions of impact.

Acknowledgements

The authors acknowledge Renault for its financial support and Dr. Trichet for his technical help.

References

Brazier-Smith, P.R., Jennings, S.G., Latham, J., 1972. The interaction of falling water drops: Coalescence. Proc. Roy. Soc. London A226, 393–408.

Brenn, G., Durst, F., Volkonko, D., 1998. On the production of satellite droplets by unstable binary drop collisions. In: International Conference on Multiphase Flow, Lyon, June 8–12, 1998.

Jiang, Y.J., Umemura, A., Law, C.K., 1991. An experiment investigation on the collision behaviour of hydrocarbon droplets. J. Fluid Mech. 234, 171–190.

Menchaca-Rocha, A., Huidodobro, F., Michaelian, H., Rodriguez, V., 1994. Disruption in liquid drop collision, I Class-94 Rouen, France, pp. 1–20.

Poo, J.Y., 1990. Coalescence and separation in binary collisions of liquid drops, Ph. D. thesis, State university of New York at Buffalo.

Qian, J., Law, C.K., 1994. Effects of liquid ambient gas properties on droplets collision. AIAA, 1–13.